

Donor Stabilized Borylnitrene: A Highly Reactive BN Analogue of Vinylidene

Holger F. Bettinger* and Holger Bornemann

Contribution from the Lehrstuhl für Organische Chemie II, Ruhr-Universität Bochum, Universitätsstr. 150, 44780 Bochum, Germany

Received February 25, 2006; E-mail: holger.bettinger@rub.de

Abstract: A donor atom stabilized borylnitrene, 2-nitreno-1,3,2-benzodioxaborole **4c**, is characterized by matrix isolation IR, UV, and ESR spectroscopy as well as multiconfiguration SCF and CI computations. UV irradiation ($\lambda = 254$ nm) of the corresponding azide **6c**, isolated in solid argon at 10 K, produces **4c** in high yield. The oxygen donor atoms in **4c** result in a triplet ground state ($|D/hc| = 1.492$ cm⁻¹, $|E/hc| = 0.004$ cm⁻¹) for the borylnitrene. The lowest energy singlet state (¹A₁) is 33 kcal mol⁻¹ higher in energy and closely related to the ground state of vinylidene. Under the conditions of matrix isolation, triplet **4c** is photochemically and thermally stable toward rearrangement to the corresponding cyclic iminoborane. Photochemical irradiation ($\lambda > 550$ nm) of **4c** rather causes an efficient reaction with molecular nitrogen, lying in matrix sites nearby, to give **6c**. Similarly, photochemical, but not thermal, trapping of **4c** with CO is possible and results in the corresponding isocyanate **9c**. Thermal reaction of **4c** with O₂ in doped argon matrixes at 35 K could be observed by IR spectroscopy to result in borylnitroso-O-oxide **17c** as shown by ¹⁸O₂ labeling experiments and DFT computations. The diradical **17c** is very photolabile and quickly rearranges to the nitritoborane **16c** upon irradiation.

Introduction

Vinylidene (**1a**) is a short-lived reactive intermediate, which quickly rearranges to acetylene (**2a**) by a prototypical [1,2]-H shift. While early photodetachment experiments¹ of the corresponding anion and semiclassical dynamics simulations² have indicated a very short lifetime of **1a**, a more recent coulomb explosion study has concluded it has a significantly longer lifetime,³ in accord with subsequent theoretical simulations of the dynamics^{4–9} based on high-level ab initio data.^{6,10,11} Fluorine substitution raises the barrier height for 1,2-migration, which is only 1.5 kcal mol⁻¹ in **1a**,¹¹ significantly,^{12,13} allowing the detection of difluorovinylidene **1b** in cryogenic matrixes.¹⁴ Carbene **1b** is extremely electrophilic and shows high reactivity,^{15–18} even toward xenon at 10 K.¹⁹

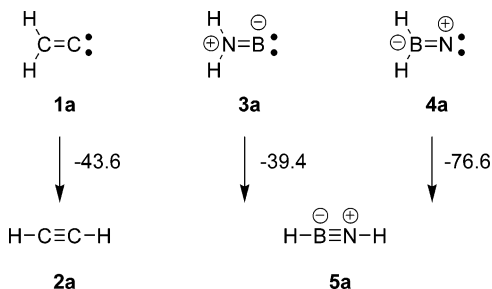
The isoelectronic relationship between C₂ and BN is very well recognized, and two BN analogues of **1**, aminoborylenes (**3**), and borylnitrenes (**4**) are conceivable. Both can rearrange by [1,2]-H migration to the BN analogues of **2**, iminoboranes **5** (Scheme 1).^{20–22}

Aminoborylene **3a** (R = H) was detected by Thompson et al.²⁴ in an argon matrix after co-deposition of laser ablated boron atoms with ammonia, while Meller and co-workers have successfully trapped derivatives of **3**.^{25–29} The barrier to [1,2]-H migration in **3a**, 27 kcal mol⁻¹ from theory, is significantly larger than that in **1a**.²² Both **1a** and **3a** have singlet ground states; the triplet state of **1a** lies significantly higher in energy.³⁰ The situation is more complex for borylnitrenes **4**. Nitrenes generally prefer triplet ground states,³¹ but the neighboring Lewis acidic boron center is expected to stabilize the singlet

- (1) Ervin, K. M.; Ho, J.; Lineberger, W. C. *J. Chem. Phys.* **1989**, *91*, 5974.
- (2) Carrington, T., Jr.; Hubbard, L. M.; Schaefer, H. F.; Miller, W. H. *J. Chem. Phys.* **1984**, *80*, 4347.
- (3) Levin, J.; Feldman, H.; Baer, A.; Ben-Hamu, D.; Heber, O.; Zajfman, D.; Vager, Z. *Phys. Rev. Lett.* **1998**, *81*, 3347.
- (4) Schork, R.; Köppel, H. *J. Chem. Phys.* **2001**, *115*, 7907.
- (5) Hayes, R. L.; Fattal, E.; Govind, N.; Carter, E. A. *J. Am. Chem. Soc.* **2001**, *123*, 641.
- (6) Zou, S.; Bowman, J. M. *Chem. Phys. Lett.* **2002**, *368*, 421.
- (7) Zou, S.; Bowman, J. M. *J. Chem. Phys.* **2002**, *117*, 5507.
- (8) Zou, S.; Bowman, J. M. *J. Chem. Phys.* **2002**, *116*, 6667.
- (9) Zou, S.; Bowman, J. M.; Brown, A. *J. Chem. Phys.* **2003**, *118*, 10012.
- (10) Stanton, J. F.; Gauss, J. *J. Chem. Phys.* **1999**, *110*, 1831.
- (11) Chang, N.-y.; Shen, M.-y.; Yu, C.-h. *J. Chem. Phys.* **1997**, *106*, 3237.
- (12) Breidung, J.; Thiel, W. *J. Mol. Spectrosc.* **2001**, *205*, 28.
- (13) Loh, Z.-H.; Field, R. W. *J. Chem. Phys.* **2003**, *118*, 4037.
- (14) Breidung, J.; Buerger, H.; Koetting, C.; Kopitzky, R.; Sander, W.; Senzlober, M.; Thiel, W.; Willner, H. *Angew. Chem., Int. Ed. Engl.* **1997**, *36*, 1983.
- (15) Koetting, C.; Sander, W.; Senzlober, M.; Buerger, H. *Chem.—Eur. J.* **1998**, *4*, 1611.
- (16) Koetting, C.; Sander, W.; Senzlober, M. *Chem.—Eur. J.* **1998**, *4*, 2360.
- (17) Sander, W.; Koetting, C. *Chem.—Eur. J.* **1999**, *5*, 24.
- (18) Koetting, C.; Sander, W. *J. Am. Chem. Soc.* **1999**, *121*, 8891.

- (19) Koetting, C.; Sander, W.; Breidung, J.; Thiel, W.; Senzlober, M.; Buerger, H. *J. Am. Chem. Soc.* **1998**, *120*, 219.
- (20) Paetzold, P. *Adv. Inorg. Chem.* **1987**, *31*, 123.
- (21) Paetzold, P. *Phosphorus, Sulfur, and Silicon* **1994**, *93–94*, 39.
- (22) Rosas-Garcia, V. M.; Crawford, T. D. *J. Chem. Phys.* **2003**, *119*, 10647.
- (23) Barreto, P. R. P.; Vilela, A. F. A.; Gargano, R. *Int. J. Quantum Chem.* **2005**, *103*, 659. These authors apparently considered a higher lying state of **4a**. The data given in Scheme 1 are for the ¹A₁ state and were computed in the present work to allow a comparison of **3a–5a** on a consistent basis.
- (24) Thompson, C. A.; Andrews, L.; Martin, J. M. L.; El-Yazal, J. *J. Phys. Chem.* **1995**, *99*, 13839.
- (25) Meller, A.; Maringgele, W.; Elter, G.; Bromm, D.; Noltemeyer, M.; Sheldrick, G. M. *Chem. Ber.* **1987**, *120*, 1437.
- (26) Meller, A.; Bromm, D.; Maringgele, W.; Boehler, D.; Elter, G. *J. Organomet. Chem.* **1988**, *347*, 11.
- (27) Maringgele, W.; Bromm, D.; Meller, A. *Tetrahedron* **1988**, *44*, 1053.
- (28) Meller, A.; Seebold, U.; Maringgele, W.; Noltemeyer, M.; Sheldrick, G. M. *J. Am. Chem. Soc.* **1989**, *111*, 8299.
- (29) Maringgele, W.; Seebold, U.; Heine, A.; Stalke, D.; Noltemeyer, M.; Sheldrick, G. M.; Meller, A. *Organometallics* **1991**, *10*, 2097.
- (30) Vacek, G.; Thomas, J. R.; DeLeeuw, B. J.; Yamaguchi, Y.; Schaefer, H. F. *J. Chem. Phys.* **1993**, *98*, 4766.

Scheme 1. Rearrangements of Vinylidene (**1a**) to Acetylene (**2a**) and of Aminoborylene (**3a**) and Borylnitrene (**4a**) to Iminoborane (**5a**) in the Isoelectronic BN Series^a



^a The $\Delta_R H(298\text{ K})$ (in kcal mol⁻¹) values, computed at the G3 level of theory, were taken from ref 23 for **3a**–**5a**.

Scheme 2. Successful Trapping of **4b** from Photolysis or Thermolysis of **6b** Was Reported by Paetzold and Coworkers (see ref 34)

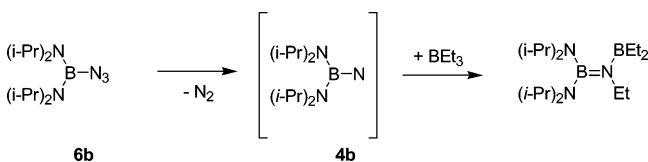
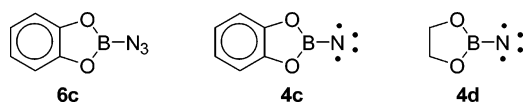


Chart 1



state (¹A₁, π^2) by interaction with its vacant boron p orbital. Indeed, previous computational investigations on parent borylnitrene **4a** have found singlet–triplet energy splittings of 12 kcal mol⁻¹ in favor of the singlet state.^{32,33} However, **4a** in its ground singlet state corresponds to a first-order stationary point on the potential energy surface in C_{2v} symmetry and relaxes to **5a** without symmetry constraint.³² This theoretical analysis is in agreement with the well-known chemistry of boronazides **6**: thermolysis or photolysis of diorgano derivatives of **6** results in iminoboranes **5**.²⁰ Borylnitrenes only could be trapped (Scheme 2) during the photolysis of diaminoazidoboranes (R₂N)₂BN₃ with bulky substituents (R = *i*Pr **6b**; R = 2,6-dimethylpiperidino).³⁴

The donor substituents at the boron atom in **4b** certainly will reduce its Lewis acidity and consequently disfavor the π^2 singlet state. However, it is unknown to which extent the relative energies of singlet and triplet states of **4** are changed by the amino substituents. Likewise, their influence on a possible barrier for the **4b** → **5b** rearrangement is unclear.

The potential stabilization of borylnitrenes by donor substituents and their expected high reactivity arising from the isoelectronic relationship to vinylidenes prompted us to investigate the photochemistry of 2-azido-1,3,2-benzodioxaborole³⁵ **6c** in cryogenic matrixes (Chart 1).

We here show that the oxygen substituents favor the triplet state of the corresponding nitrene **4c**, allowing the spectroscopic characterization of a borylnitrene for the first time. Matrix

Table 1. Relative Energies (in kcal mol⁻¹) Computed for Low-Lying Electronic States of **4a** and **4c** at Various Levels of Theory Using the cc-pVTZ Basis Set

species	config	n,m	(n,m)-CASSCF	CISD ^a	CISD+Q ^a	CCSD(T)
³ A ₂ - 4a	$\sigma^1\pi^1$	10,10	0	0 ^b	0 ^b	0
¹ A ₁ - 4a	π^2	10,10	-9.0	-7.7 ^b	-7.2 ^b	-7.1
¹ A ₂ - 4a	$\sigma^1\pi^1$	10,10	33.0	28.8 ^b	28.4 ^b	n.a.
³ A ₂ - 4c	$\sigma^1\pi^1$	12,11	0	0	0	0 ^d
¹ A ₁ - 4c	π^2	12,11	37.0	33.9 ^c	32.7 ^c	34.9 ^d
¹ A ₂ - 4c	$\sigma^1\pi^1$	12,11	37.8	35.3	34.1	n.a.
³ A- 4d	$\sigma^1\pi^1$	6,5	0	0	0	0
¹ A- 4d	π^2	6,5	36.5	32.9	31.8	n.a.

^a Based on (n,m)-CASSCF geometries, which were obtained using the cc-pVTZ basis set for **4a**, and the 6-31G* basis set for **4c** and **4d**. ^b Using a full-valence (10,10) multiconfiguration reference. ^c Using a two-configuration reference. ^d Using the (12,11)-CASSCF/6-31G* geometries.

isolation studies of **4c** reveal an unprecedented high thermal reactivity with molecular oxygen already at temperatures as low as 35 K and a high photochemical reactivity with nitrogen and carbon monoxide.

Results and Discussion

Electronic and Geometric Structures of 4a and 4c. To shed light on the influences of substituents on the relative energies of singlet and triplet states in borylnitrenes, multiconfiguration and coupled-cluster computations were performed. The lowest energy state of **4c** is a triplet T₀ of A₂ symmetry with a $\sigma^1\pi^1$ [(12b₂)¹ (4b₁)¹] configuration. The S₁ state (A₁ symmetry) is 33 kcal mol⁻¹ higher in energy (see Table 1) and can be characterized as π^2 . This state has a large two-configuration character as evidenced by the reference coefficients of 0.757 (π^2) and -0.475 (σ^2) from TC-CISD/cc-pVTZ and by the (12,11)-CASSCF natural orbital occupation numbers of 1.37 (4b₁) and 0.63 (12b₂). Note that the CCSD(T)/cc-pVTZ energy for the S₁ state of **4c** is in reasonably good agreement with the CI data.

The energetic ordering of electronic states contrasts that of the parent borylnitrene H₂BN **4a**. Our multireference CI computations (based on full valence complete active spaces) place the π^2 state below the triplet state of $\sigma^1\pi^1$ configuration (A₂ symmetry) by 7 kcal mol⁻¹. This singlet–triplet splitting is smaller than the 12 kcal mol⁻¹ derived by McKee from G2 computations³³ and the 31 kcal mol⁻¹ (UHF/6-31G*) reported by Nguyen,³² who considered the higher-lying ³B₂ state of **4a**. The presence of the two oxygen donor substituents in **4c** reduces the Lewis acidity of boron and thus *reverses* the energetic ordering of singlet and triplet states compared to parent **4a**. A very similar singlet–triplet energy splitting of 32–33 kcal mol⁻¹ is obtained for the parent C₂ symmetric 2-nitreno-1,3,2-dioxaborole **4d** (see Chart 1), indicating that the potential aromatic nature of the five-membered ring in **4c** is not responsible for the destabilization of the singlet state.

The S₂ state of **4c** is 34 kcal mol⁻¹ above T₀ in energy and thus energetically similar to S₁. The S₂ state has the same configuration as the T₀ state and is thus of A₂ symmetry. Due to the two-determinant nature of the S₂ state, we were unable to obtain coupled cluster data.

Note that this $\sigma^1\pi^1$ state is the lowest energy singlet state in prototypical phenyl nitrene, 16 kcal mol⁻¹ above the triplet ground state,³⁶ while the π^2 state corresponds to S₃. Hence, the

(31) Platz, M. S. In *Reactive Intermediate Chemistry*; Moss, R. A., Platz, M. S., Jones, M., Eds.; Wiley-Interscience: Hoboken, NJ, 2004; p 501.

(32) Nguyen, M. T. *J. Chem. Soc., Chem. Commun.* **1987**, 342.

(33) McKee, M. L. *J. Phys. Chem.* **1994**, *98*, 13243.

(34) Pieper, W.; Schmitz, D.; Paetzold, P. *Chem. Ber.* **1981**, *114*, 3801.

(35) Fraenk, W.; Haberer, T.; Klapötke, T. M.; Nöth, H.; Polborn, K. *J. Chem. Soc., Dalton Trans.* **1999**, 4283.

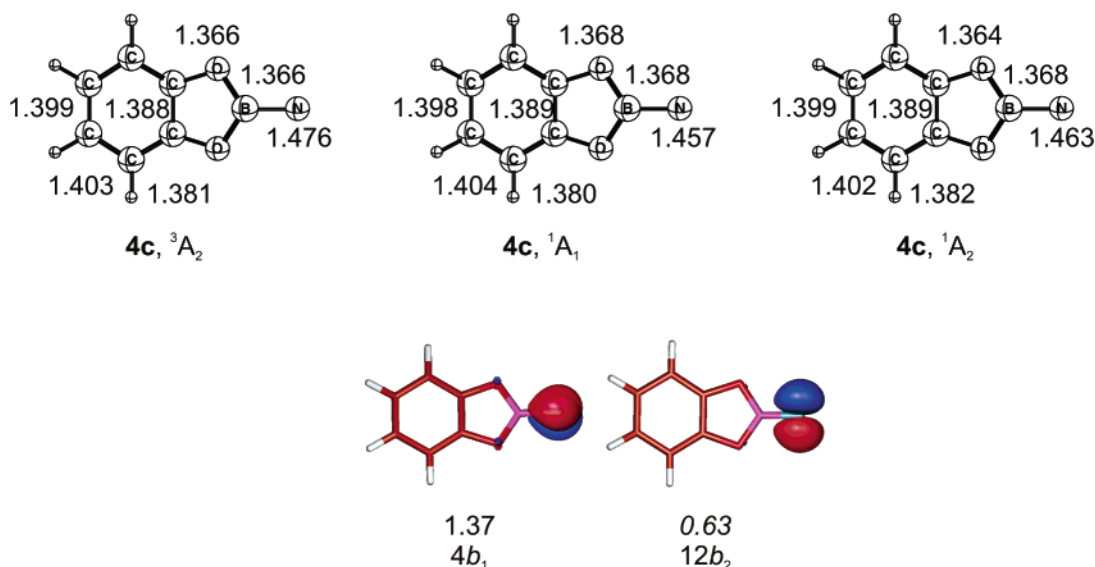


Figure 1. Geometries of the three lowest energy states of **4c** as computed at the (12,11)-CASSCF/6-31G* level of theory. Bond lengths are given in angstrom. The $4b_1$ and $12b_2$ natural orbitals and their occupation numbers computed at this level of theory are also given for the 1A_1 state of **4c**.

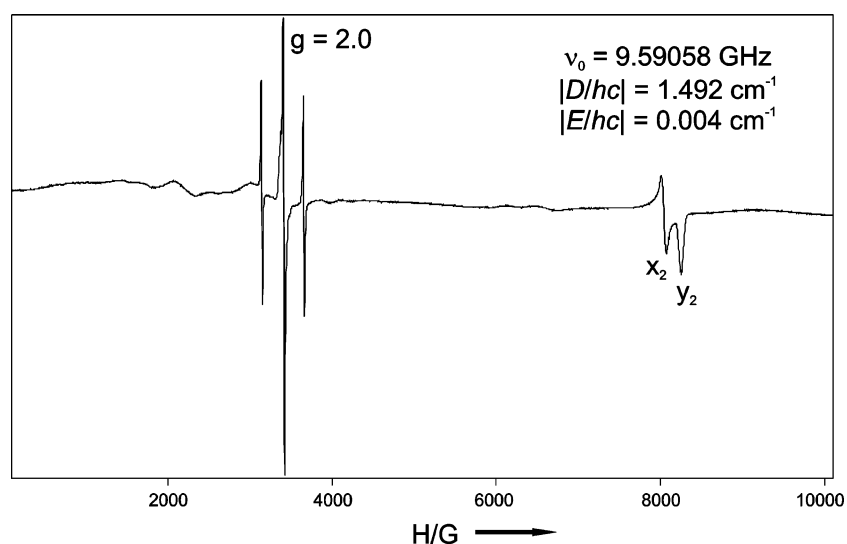


Figure 2. ESR spectrum of triplet 2-nitreno-1,3,2-benzodioxaborole **4c** photolytically generated from 2-azido-1,3,2-benzodioxaborole **6c** in an argon matrix at 10 K.

ordering of electronic states in **4c** differs significantly from that of the well-characterized aryl nitrenes.

The geometric parameters of the three states of **4c** considered show the expected characteristics (Figure 1). In particular, the B–N bond lengths obtained from CASSCF computations decrease from 1.476 Å (3A_2) to 1.463 Å (1A_2) and to 1.457 Å (1A_1), in agreement with the somewhat increased π interaction in S_1 .

In summary, the electronic structure of **4c** is characterized by a triplet ground state. The lowest energy singlet state is of a closed-shell nature, and thus it is isoelectronic to, and has the same configuration as, the ground state of vinylidene.

Generation and Direct Spectroscopic Characterization of 2-Nitreno-1,3,2-benzodioxaborole 4c by ESR, IR, and UV Spectroscopies. UV-light irradiation (254 nm) of **6c** isolated in solid argon at 10 K within the cavity of an ESR spectrometer gives rise to an intense absorption with a shape characteristic

for an electronic triplet state (Figure 2). The values of the corresponding zero-field splitting parameters, $|D/hc| = 1.492$ and $|E/hc| = 0.004$ cm $^{-1}$, are in the range that is typical for aryl nitrenes.³⁷ The larger D value, compared to that of aryl nitrenes, is indicative of a limited delocalization in the triplet state. The E value of **4c** is particularly large for a C_{2v} symmetric nitrene, but large E values have also been observed by Wentrup's group for 2-pyrimidinyl nitrenes,^{38,39} possibly due to unusually large spin–orbit coupling.

Following the same experiment by IR spectroscopy shows that 254-nm irradiation of **6c** results in the complete disappearance of its IR bands, and a set of new IR absorptions can be detected (Figure 3). The most intense bands are located at 1470, 1230, 809, and 745 cm $^{-1}$. In addition, a number of bands are

(37) Platz, M. S. In *CRC Handbook of Organic Photochemistry*; Scaiano, J. C., Ed.; CRC Press: Boca Raton, FL, 1989; Vol. 2, p 373.

(38) Kuzaj, M.; Lüerssen, H.; Wentrup, C. *Angew. Chem., Int. Ed. Engl.* **1986**, *25*, 480.

(39) Kvaskoff, D.; Bednarek, P.; George, L.; Waich, K.; Wentrup, C. *J. Org. Chem.* **2006**, *71*, 4049.

(36) Bettinger, H. F.; Sander, W. *J. Am. Chem. Soc.* **2002**, *125*, 9726.

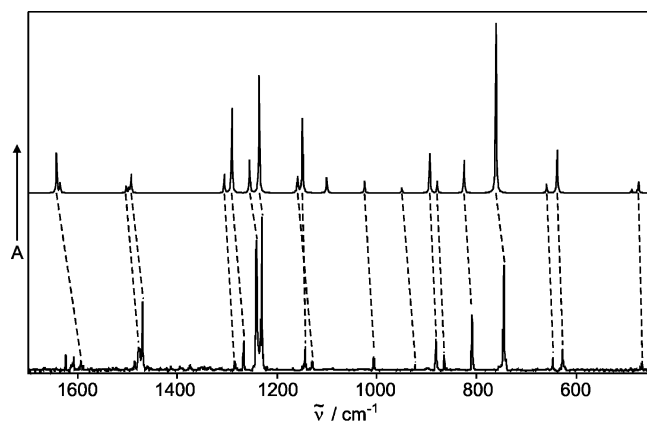


Figure 3. (Bottom) IR spectrum (in absorbance) of 2-nitreno-1,3,2-benzodioxaborole **4c**, matrix-isolated in argon at 10 K. The nitrene was generated by 254-nm irradiation of azide **6c**. (Top) IR spectrum of the ^{10}B - and ^{11}B -isotopomers of **4c** as calculated at the UB3LYP/6-311+G(d,p) level of theory.

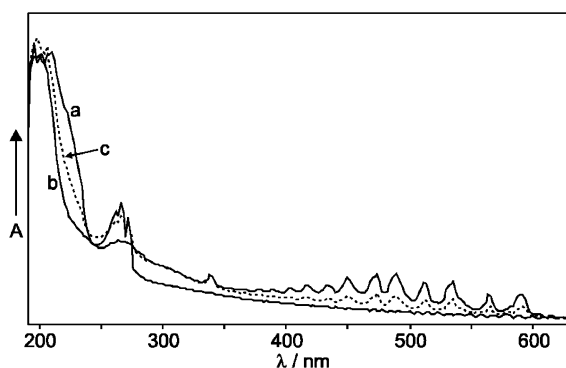


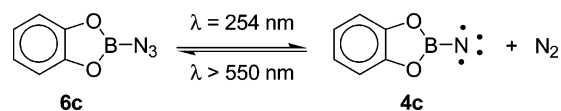
Figure 4. UV-vis spectra showing the photochemistry of 2-azido-1,3,2-benzodioxaborole **6c**. (a) Spectrum of **6c**, matrix-isolated in argon at 10 K. (b) Same spectrum after 254 nm irradiation resulting in nitrene **4c**. (c) Same spectrum after subsequent 550 nm irradiation. **6c** has been partly regenerated.

accompanied by features at higher vibrational frequencies having roughly one-fifth of the intensity of the parent peaks. This intensity ratio is typical for samples with natural boron isotope composition (^{10}B : ^{11}B = 1:4), and hence these bands are due to modes involving the boron atom.⁴⁰ Comparison with computed data shows qualitative agreement of the vibrational frequencies, intensities, and boron isotopic shifts with the triplet nitrene **4c** (see Supporting Information, Table S1). This assignment is supported by the ESR data mentioned above, and also by UV spectroscopy as discussed below.

Photochemical decomposition of **6c** with 254-nm irradiation results in an intense orange-red color of the matrix, which was colorless initially. The UV/vis spectral analysis of the 254-nm photolysis of **6c** shows that its structured absorption maximum at 261–272 nm gradually decreases while new absorptions grow in. The spectrum obtained after complete decomposition of the azide **6c** shows absorptions at 264 nm as well as a number of bands with pronounced vibrational progression extending from 377 nm up to 591 nm (Figure 4). The absorptions between 377 and 450 nm show a very regular average spacing of 880 cm^{-1} ,

(40) A band in the BO stretching region at 1243 cm^{-1} is tentatively assigned to the ^{10}B isotopomer, but its intensity is too large. There is also an unidentified species formed during UV photolysis characterized by a 340-nm absorption in the UV spectra, and this byproduct could possibly also absorb in the BO stretching region. For possible rearrangements of **4c**, see Supporting Information.

Scheme 3. Wavelength Dependent Photostationary Equilibrium between **6c** and **4c**



indicating that this part of the spectrum is dominated by a vibrational progression involving a 880 cm^{-1} mode of an excited state of **4c**.

Between 450 and 590 nm, the spacing of UV bands is no longer regular, complicating the distinction between vibrational progressions and electronic transitions. The computational analysis (TD-UB3LYP/6-311+G(d,p)) of the excited states of $^3\text{A}_2$ -**4c** arrives at four excited states with nonzero transition moments above 400 nm: 1B_2 (526 nm); 1A_1 (523 nm); 1B_1 (496 nm); 2B_2 (437 nm). All these are one-electron transitions and involve either excitations from the benzene π system into the $\text{N}(\pi)$ orbital to give the 1B_1 and 1A_2 excited states or from the nitrogen lone pair to the $\text{N}(\pi)$ and $\text{N}(\sigma)$ orbitals to give the 1B_2 and 2B_1 states, respectively.

When we sought to incite rearrangements of **4c** by irradiating into the low-energy absorptions identified in the UV experiments with visible light ($\lambda > 550\text{ nm}$), we were quite surprised to find that this irradiation resulted in the regeneration of **6c** in high yield ($\sim 50\%$), as shown by IR (Figure S2 in the Supporting Information) and UV spectroscopy. Also in the ESR spectrum the absorptions due to **4c** reduce in intensity upon visible light irradiation. No new IR, UV, or ESR absorptions are observed. The reaction with nitrogen upon irradiation in cryogenic matrixes has been observed previously by Hayes and Sheridan for phenylnitrene,⁴¹ Azide formation is only a minor side reaction of phenylnitrene, which largely undergoes a rearrangement reaction. The very efficient reaction of **4c** with molecular nitrogen at cryogenic temperatures is without precedence. This reaction is not quantitative because some of the nitrogen conceivably has diffused away from **4c** during its photochemical generation and is thus not available for the reaction back to **6c** (Scheme 3). This explanation is in agreement with annealing experiments. After warming the matrix to 35 K for 10 min, the amount of **6c** formed upon subsequent long-wavelength irradiation is reduced to approximately 10% of the original concentration.

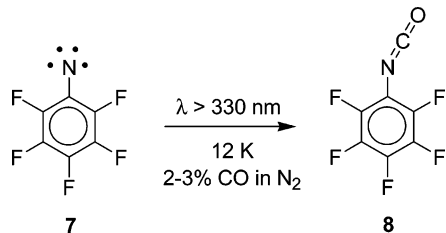
Interestingly, long-wavelength irradiation of **4c** isolated in solid nitrogen at 10 K only produces small amounts of the azide **6c** ($\sim 10\%$). Warming the matrix to 20 K during the photolysis results in a significantly improved yield of **6c** ($\sim 50\%$). The reversible azide cleavage then could be employed for trapping with labeled dinitrogen, $^{15}\text{N}_2$. Visible light irradiation of **4c** in nitrogen matrixes doped with 2% $^{15}\text{N}_2$ at 20 K resulted in an intense band at 2099 cm^{-1} due to $^{15}\text{N}_2$ -**6c**. This observed isotopic shift of -73 cm^{-1} is in good agreement with the one computed (-74 cm^{-1}) for $^{15}\text{N}_2$ -**6c**.

Reaction with CO. Motivated by the high reactivity of **4c** toward nitrogen upon visible light irradiation, we investigated the trapping of **4c** with CO. While the CO molecule is well-known in carbene chemistry to react under cryogenic conditions with carbenes in their singlet and triplet states to give ketenes,⁴² the analogous reaction with nitrenes has only been considered

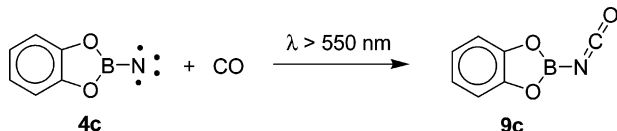
(41) Hayes, J. C.; Sheridan, R. S. *J. Am. Chem. Soc.* **1990**, *112*, 5879.

(42) Sander, W.; Bucher, G.; Wierlacher, S. *Chem. Rev.* **1993**, *93*, 1583.

Scheme 4. Pentafluorophenyl nitrene **7** Has Been Shown to React Photochemically in a CO Doped Nitrogen Matrix to the Isocyanate **8** (see ref 43)



Scheme 5. Photochemical Excitation of Borylnitrene **4c** in CO Doped Argon Matrix ($\leq 1.5\%$ CO) Results in Formation of Isocyanate **9c**



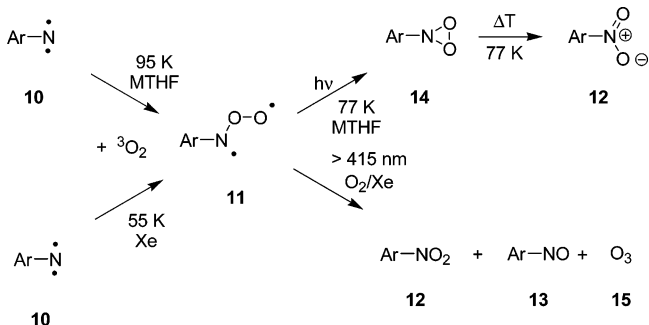
occasionally. Dunkin and Thomson have shown that the highly reactive pentafluorophenyl nitrene **7** reacts photochemically, but not thermally at 35 K, in a CO doped nitrogen matrix to the corresponding isocyanate **8** (Scheme 4).⁴³

We can observe the analogous reaction for **4c**. Irradiation of **6c** isolated in an argon matrix containing up to 1.5% of CO results in formation of **4c** along with a new compound with strong absorptions at 2301, 1569 (broad), 1474, 1239 (broad and split), and 617 cm^{-1} . Based on the IR spectral data reported by Lappert and Pyszora⁴⁴ for isocyanate **9c** (in the liquid phase: 2278 vs, 1553 vs, 1463 vs, 1255 vs, 614 s) and B3LYP computations (Table S2), the new compound is assigned to **9c**. As expected, **4c** does not react with CO upon annealing of the matrix to 35 K, while visible light irradiation ($\lambda > 550 \text{ nm}$) of **4c** at 10 K does yield **9c** from reaction with CO (Scheme 5), in addition to some azide **6c**, which forms from the reaction with nitrogen.

Reaction with O₂. While O₂, which has a triplet ground state, reacts rapidly with triplet carbenes,⁴⁵ even at the temperatures accessible within argon matrixes,^{46,47} reactions with triplet nitrenes are much slower.^{48–52} Nonetheless, matrix isolation IR studies of Laursen et al. show that the imidogen radical NH can thermally be oxidized in xenon at 50 K to give the corresponding nitroso-*O*-oxide HNOO, which rearranges photochemically to nitrous acid, HONO.⁵³

The photooxidation of aryl nitrenes **10** with molecular oxygen, studied in glasses and in solution at room temperature, involves nitroso-*O*-oxides **11**, which rearrange to the corresponding nitro compounds (**12**) or transfer one oxygen atom to substrates, thereby yielding nitroso compounds **13**.^{48,54} The decay kinetics

Scheme 6. Thermal and Photooxidation of Aryl Nitrenes **10** in Organic Glasses (Top Path) and Xenon Matrixes (Bottom Path) (see refs 60 and 61)



of nitroso-*O*-oxides were recently studied by Safiullin's group using flash photolysis.^{55–59} The detailed UV/vis studies of Harder et al.⁶⁰ in organic glasses show that **10** react thermally with O₂ at 95 K to give the corresponding **11**. These react photochemically at 77 K to dioxaziridines **14**, which only have a short lifetime ($\tau_{1/2} \approx 4 \text{ min}$) under these conditions and thermally rearrange to the corresponding nitro compounds (Scheme 6, top pathway).⁶⁰

IR spectroscopic analysis of the photooxidation of *p*-nitrophenyl nitrene was very recently achieved by Inui et al. in solid xenon doped with 5% O₂ at 50 K.⁶¹ Following the thermal oxidation of **10** with ³O₂ to **11**, subsequent photochemical reactions result in formation of aryl nitro **12** and aryl nitroso **13** compounds along with some ozone **15** (Scheme 6, bottom pathway).⁶¹ No **14** was detected under these conditions. The formation of **13** and **15** was considered evidence for the photochemical cleavage of the O–O bond in **11**, while **12** was assumed to result from the reaction of oxygen atom with **13**.

The 254-nm irradiation of **6c** in the presence of oxygen (0.5–1.0%) resulted in **4c** and one new set of IR bands, termed A and characterized by 1752, 1410, 1336, 1235, and 632 cm^{-1} absorptions. Subsequent annealing of the matrix to 35 K produces another set, termed B and characterized by 1375, 1302, 1119, and 924 cm^{-1} absorptions.

Under these conditions set A does not change in intensity, but the bands due to **4c** reduce. Hence, B is the product of the thermal reaction of ground-state oxygen with **4c**. Finally, 254-nm irradiation of the matrix after annealing causes an increase of signals A and a complete disappearance of signals assigned to B.

To support any assignments to species A and B we have also performed experiments with ¹⁸O₂. Set A has now characteristic signals (¹⁸O shifts in cm^{-1} are given in parentheses) at 1707 cm^{-1} (expt: –45; calcd: –49), 1397 (expt: –13; calcd: –10), 751 cm^{-1} (expt: –15; calcd: –15), 622 (expt: –10; calcd: –11). After annealing, new bands due to B are observed at 1058 cm^{-1} (expt: –61; calcd: –55), 916 cm^{-1} (expt: –8; calcd: –11).

(43) Dunkin, I. R.; Thomson, P. C. P. *J. Chem. Soc., Chem. Commun.* **1982**, 1192.

(44) Lappert, M. F.; Pyszora, H. *J. Chem. Soc. A* **1967**, 854.

(45) Bucher, G.; Scaiano, J. C.; Platz, M. S. *Landolt-Börnstein, Group II, Volume 18, Subvolume E2*; Springer: Berlin, 1998.

(46) Sander, W. *Angew. Chem., Int. Ed. Engl.* **1986**, 25, 255.

(47) Sander, W. *Angew. Chem., Int. Ed. Engl.* **1990**, 29, 344.

(48) Brinen, J. S.; Singh, B. *J. Am. Chem. Soc.* **1971**, 93, 6623.

(49) Gritsan, N. P.; Pritchina, E. A. *J. Inf. Rec. Mater.* **1989**, 17, 391.

(50) Pritchina, E. A.; Gritsan, N. P. *J. Photochem. Photobiol., A* **1988**, 43, 165.

(51) Liang, T.-Y.; Schuster, G. B. *J. Am. Chem. Soc.* **1987**, 109, 7803.

(52) Liu, J.; Hadad, C. M.; Platz, M. S. *Org. Lett.* **2005**, 7, 549.

(53) Laursen, S. L.; Grace, J. E.; DeKock, R. L.; Spronk, S. A. *J. Am. Chem. Soc.* **1998**, 120, 12583.

(54) Ishikawa, S.; Nojima, T.; Sawaki, Y. *J. Chem. Soc., Perkin Trans. 2* **1996**, 127.

(55) Chainikova, E. M.; Khursan, S. L.; Safiullin, R. L. *Dokl. Phys. Chem.* **2003**, 390, 163.

(56) Safiullin, R. L.; Khursan, S. L.; Chainikova, E. M.; Danilov, V. T. *Kinet. Catal.* **2004**, 45, 640.

(57) Chainikova, E. M.; Khursan, S. L.; Safiullin, R. L. *Dokl. Phys. Chem.* **2004**, 396, 138.

(58) Chainikova, E. M.; Khursan, S. L.; Safiullin, R. L. *Kinet. Catal.* **2004**, 45, 794.

(59) Chainikova, E. M.; Khursan, S. L.; Safiullin, R. L. *Dokl. Phys. Chem.* **2005**, 403, 133.

(60) Harder, T.; Wessig, P.; Bendig, J.; Stösser, R. *J. Am. Chem. Soc.* **1999**, 121, 6580.

(61) Inui, H.; Irisawa, M.; Oishi, S. *Chem. Lett.* **2005**, 34, 478.

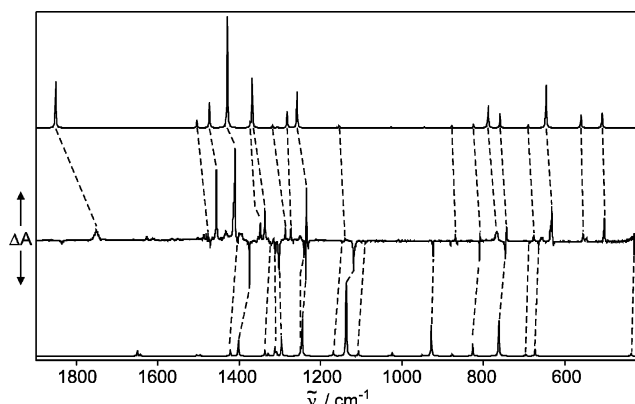


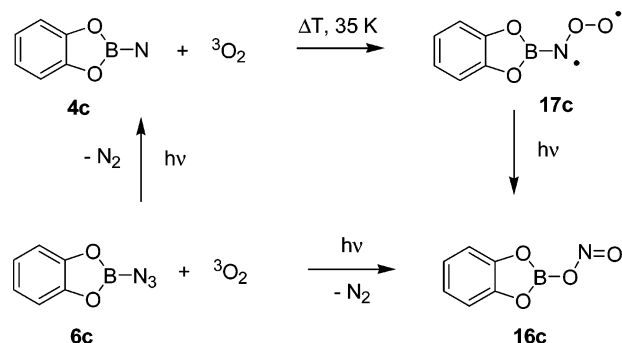
Figure 5. (Center) Difference IR spectrum showing the photochemistry (254 nm irradiation) of nitroso-*O*-oxide **17c**. Bands pointing downward are disappearing during the irradiation and assigned to **17c**; bands pointing upward are appearing and assigned to nitritoborane **16c**. (Bottom) IR spectrum of the ^{10}B - and ^{11}B -isotopomer of **17c**, respectively, calculated at the UB3LYP/6-311+G(d,p) level of theory. (Top) IR spectrum of the ^{10}B - and ^{11}B -isotopomer of **16c**, respectively, calculated at the B3LYP/6-311+G(d,p) level of theory.

Comparison of the experimental vibrational frequencies, intensities, and oxygen and boron isotope shifts with B3LYP data allows assignment of species A to the nitritoborane **16c** and of species B to nitroso-*O*-oxide **17c** (Figure 5, Tables S3 and S4).

We could identify computationally three conformers of **17c** (Figure 6), but the experimental vibrational data are only in agreement with the thermodynamically most stable anti conformer. Likewise, the final product of photooxidation of **4c**, nitritoborane **16c**, is thermodynamically more stable than dioxaziridine **18c** and nitroborane **19c** by 104 and 22 kcal mol $^{-1}$. The spectroscopic data of **18c** and **19c** is not compatible with set A (see Figure S4 in the Supporting Information); these two isomers cannot be observed in our experiments. The oxidation of boryl nitrene in an argon matrix can thus be summarized as shown in Scheme 7.

In view of the known reactivity of aryl nitrenes, borylnitrene **4c** is remarkable for two reasons: first, it reacts thermally with oxygen already at 35 K in an argon matrix, and second, its

Scheme 7. Thermal and Photooxidation of Borylnitrene **4c** Yields Nitritoborane **16c**



nitroso-*O*-oxide behaves qualitatively different upon photoexcitation. The formal insertion of oxygen into the bond involving the nitrene nitrogen has never been observed in any aryl nitrene studied previously. The different final reaction product of photooxidation of borylnitrene **4c** is due to the possibility of forming a strong B–O bond in **9c**.

Conclusions

The present investigation of azide **6c** allows for the first time the characterization of a borylnitrene using matrix isolation IR, UV, and ESR spectroscopies and observation of its reactions with the small diatomic molecules nitrogen, carbon monoxide, and oxygen. We can draw the following conclusions from our study of donor substituted borylnitrenes.

1. The presence of the oxygen donor atoms in nitreno-1,3,2-benzodioxaborol **4c** changes the spin multiplicity of the electronic ground state from singlet as in parent H₂BN (**4a**) to triplet. The lowest energy singlet state of **4c** is 33 kcal mol $^{-1}$ above the triplet in energy and has the same leading electronic configuration as the ground state of vinylidene (**1a**). However, the multiconfiguration character in **4c** is significantly enhanced compared to **1a**.

2. While the lowest energy singlet state of **4a** is a first-order saddle point and relaxes to iminoborane, the strong B–O bonds

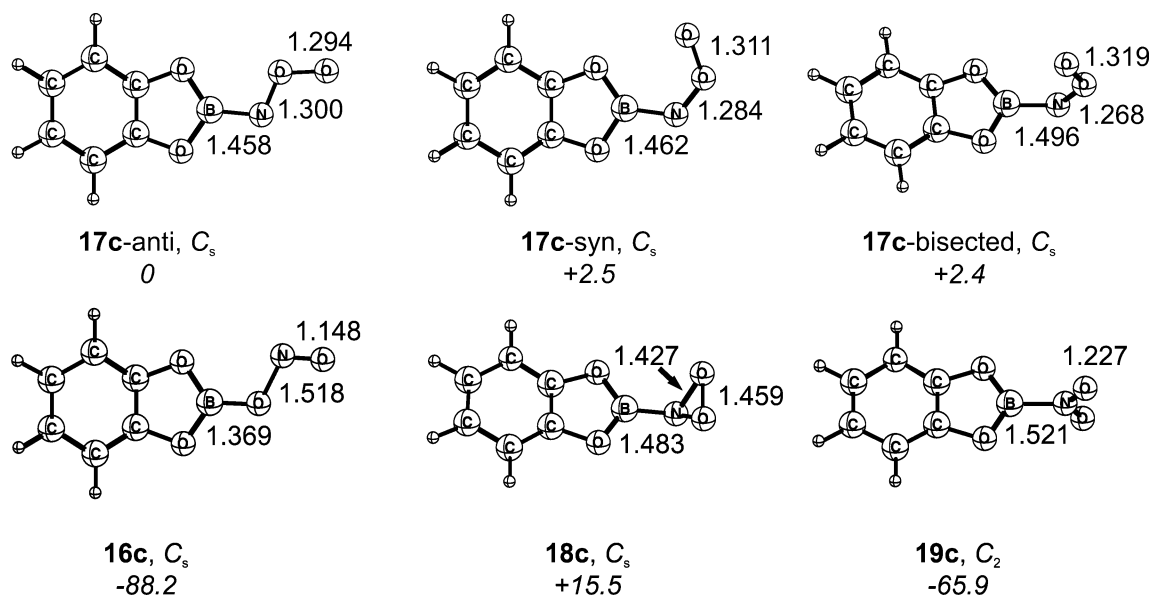


Figure 6. Structures of possible products of the reaction of borylnitrene **4c** with dioxygen as computed at the (U)B3LYP/6-311+G(d,p) level of theory. Selected bond lengths are given in angstrom, and relative energies (in kcal mol $^{-1}$) are given in italics and are corrected for zero-point vibrational energies.

stabilize the singlet state of **4c** and turn it into a minimum on the potential energy surface.

3. As a consequence of the electronic structure described above, **4c** can be generated photochemically from the corresponding azide **6c** and characterized in its triplet electronic ground state by matrix isolation IR, UV, and ESR spectroscopies.

4. While **4c** appears to be stable to rearrangements upon photophysical excitation, it reacts with molecular nitrogen (either in argon or nitrogen matrixes) and carbon monoxide (in doped argon matrixes) to the azide **6c** and the isocyanate **9c** upon visible light irradiation. No reaction, on the other hand, with these diatomic molecules is observed upon annealing of the matrix to 35 K.

5. In O₂ doped argon matrixes **4c** is reacting thermally with oxygen at 35 K to give the corresponding nitroso-*O*-oxide **17c**. This high reactivity is unusual for nitrenes, which generally do not react with ground-state molecular oxygen at temperatures as low as 35 K. The nitroso-*O*-oxide, in turn, is very photolabile and rearranges to the nitritoborane **16c**.

Experimental Section

Computations. Density functional theory (DFT) computations using the B3LYP^{62,63} functional in conjunction with the 6-311+G(d,p) basis set were employed for optimization of geometries and for computing the harmonic vibrational frequencies of **4c** and of possible products of reactions with trapping agents. The spin-unrestricted formalism was used for singlet states if the spin-restricted solutions turned out to have a triplet instability.⁶⁴ The excited states of triplet **4c** were investigated at the geometry optimized at the UB3LYP/6-311+G** level using time-dependent (TD) density functional response theory in conjunction with the UB3LYP functional and the 6-311+G** basis set, i.e., TD-UB3LYP/6-311+G**.⁶⁵

The electronic structure of **4** and some of its singlet states were considered further by complete-active space SCF (CASSCF) computations and the 6-31G* basis set. The parent boryl nitrene **4a** was investigated using a full-valence active space, i.e., (10,10)-CASSCF. The active spaces used for **4c** consisted of the complete π systems and the in-plane p-type orbital at the nitrene center resulting in 12 electrons and 11 orbitals, i.e., (12,11)-CASSCF. The geometries were fully optimized using analytic gradients, and harmonic vibrational frequencies were obtained for the lowest energy triplet and singlet states by finite differences of analytic gradients.

The relative energies were refined by subsequent internally contracted multireference-configuration interaction computations including single and double excitations (CISD);^{66,67} the effects of unlinked quadruple excitations were considered via Davidson's correction (CISD+Q).^{68,69} The reference configurations are based on the (10,10)-CASSCF wave function in the case of **4a**, but only on (2,2)-CASSCF wave functions for **4c** due to computational limitations. The CISD computations are thus of a single reference nature for the triplet and open-shell singlet states (³A₂ and ¹A₂) and of a two-configuration nature for the closed-shell singlet state of **4c**. The closed-shell singlet and the triplet states of **4a** and **4c** were also computed using coupled cluster theory with

single, double, and a perturbative estimate of connected triple excitations [CCSD(T)].^{70–72} The partially spin-restricted open-shell coupled cluster theory [RHF-RCCSD(T)] was employed for triplet electronic states.⁷³ Dunning's cc-pVTZ basis set was utilized in all single-point computations.⁷⁴ The frozen-core approximation was employed for all electron correlated ab initio methods. All CASSCF, CI, and CCSD(T) computations were performed with MOLPRO,⁷⁵ while Gaussian 03 was employed for B3LYP theory.⁷⁶ Molecular orbitals were plotted using MOLDEN.⁷⁷

Materials and Matrix Isolation Spectroscopy. 2-Azido-1,3,2-benzodioxaborole **6c** was synthesized according to the published procedure.³⁵ Matrix isolation experiments were performed by standard techniques using an APD CSW-202 Displex closed cycle helium cryostat. Matrixes were produced by deposition of argon (Messer Griesheim, 99.9999%), mixtures of argon and oxygen (Messer Griesheim, 99.998%) or carbon monoxide (Union Carbide, research purity), nitrogen (Messer Griesheim, 99.9999%) or mixtures of nitrogen and ¹⁵N₂ (Isotec, min. 98 atom-% ¹⁵N) on top of a CsI (IR) or sapphire (UV/vis) window at 30 K. Infrared spectra were recorded using a Bruker IFS66 FTIR spectrometer with a standard resolution of 0.5 cm⁻¹ in the range 400–4000 cm⁻¹. UV/vis spectra were recorded on a Hewlett-Packard 8452A diode array spectrophotometer with a resolution of 2 nm. ESR spectra were measured with a Bruker EleXsys E500 spectrometer. The computer simulation of the ESR spectrum of **4c** was performed using the Xsophe computer simulation software suite (version 1.0.4),⁷⁸ developed by the Centre for Magnetic Resonance and Department of Mathematics, University of Queensland, Brisbane (Australia) and Bruker Analytik GmbH, Rheinstetten (Germany). The simulation was performed by using a matrix diagonalization method for *S* = 1 and setting the parameters 9.59058 GHz, 2.003, *D*/*h**c* = 1.492 cm⁻¹ and *E*/*h**c* = 0.004 cm⁻¹. Irradiations were carried out using a low-pressure mercury lamp (λ = 254 nm, Grätzel) or Osram HBO 500 W/2 mercury high-pressure arc lamps in Oriel housings equipped with quartz optics. IR irradiation from the lamps was absorbed by a 10-cm path of water. For wavelength selection, dichroic mirrors ("cold mirrors") in combination with Schott cutoff filters (50% transmission at the wavelength specified) were used.

Acknowledgment. This work was supported by the DFG. We thank Priv.-Doz. Dr. Götz Bucher, Prof. Dr. C. Wentrup, and Prof. R. S. Sheridan for stimulating discussions, Prof. W. Sander for access to the matrix isolation equipment, and Dipl.-Chem. Dirk Grote and Klaus Gomann for performing the ESR experiments.

Supporting Information Available: Tables S2–S4 with experimental and computed vibrational frequencies, Cartesian coordinates and absolute energies for all species considered, complete refs 75 and 76, experimental IR spectra (N₂ reaction, CO trapping), computed IR spectra for **18c** and **19c**, and simulation of the ESR spectrum of **4c**. This material is available free of charge via the Internet at <http://pubs.acs.org>.

JA061346Y

(62) Becke, A. D. *J. Chem. Phys.* **1993**, *98*, 5648.

(63) Lee, C.; Yang, W.; Parr, R. G. *Phys. Rev. B* **1988**, *37*, 785.

(64) Bauernschmitt, R.; Ahlrichs, R. *J. Chem. Phys.* **1996**, *104*, 9047.

(65) Stratmann, R. E.; Scuseria, G. E.; Frisch, M. J. *J. Chem. Phys.* **1998**, *109*, 8218.

(66) Werner, H.-J.; Knowles, P. J. *J. Chem. Phys.* **1988**, *89*, 5803.

(67) Knowles, P. J.; Werner, H.-J. *Chem. Phys. Lett.* **1988**, *145*, 514.

(68) Langhoff, S. R.; Davidson, E. R. *Int. J. Quantum Chem.* **1974**, *8*, 61.

(69) Duch, W.; Diercksen, G. H. F. *J. Chem. Phys.* **1994**, *101*, 3018.

(70) Purvis, G. D.; Bartlett, R. J. *J. Chem. Phys.* **1982**, *76*, 1910.

(71) Raghavachari, K.; Trucks, G. W.; Pople, J. A.; Head-Gordon, M. *Chem. Phys. Lett.* **1989**, *157*, 479.

(72) Hampel, C.; Peterson, K.; Werner, H.-J. *Chem. Phys. Lett.* **1992**, *190*, 1.

(73) Knowles, P. J.; Hampel, C.; Werner, H.-J. *J. Chem. Phys.* **1993**, *99*, 5129.

(74) Dunning, T. H. *J. Chem. Phys.* **1989**, *90*, 1007.

(75) Amos, R. D. et al. MOLPRO, a package of ab initio programs designed by H.-J. Werner and P. J. Knowles, version 2002.1.

(76) Frisch, M. J. et al. Gaussian 03, revision B.4; Pittsburgh, PA, 2003.

(77) Schaftenaar, G.; Noordik, J. H. *J. Comput.-Aided Mol. Des.* **2000**, *14*, 123.

(78) Griffin, M.; Muys, A.; Noble, C.; Wang, D.; Eldershaw, C.; Gates, K. E.; Burrage, K.; Hanson, G. R. *Mol. Phys. Rep.* **1999**, *26*, 6084.